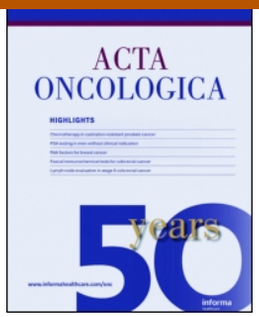

Acta Oncologica

ISSN: 0284-186X (Print) 1651-226X (Online) Journal homepage: https://www.tandfonline.com/loi/ionc20

Daily adaptive proton therapy – the key to innovative planning approaches for paranasal cancer treatments

Lena Nenoff, Michael Matter, Johanna Hedlund Lindmar, Damien Charles Weber, Antony John Lomax & Francesca Albertini

To cite this article: Lena Nenoff, Michael Matter, Johanna Hedlund Lindmar, Damien Charles Weber, Antony John Lomax & Francesca Albertini (2019): Daily adaptive proton therapy – the key to innovative planning approaches for paranasal cancer treatments, Acta Oncologica, DOI: 10.1080/0284186X.2019.1641217

To link to this article: https://doi.org/10.1080/0284186X.2019.1641217

ACTA ONCOLOGICA
https://doi.org/10.1080/0284186X.2019.1641217

Taylor & Francis
Taylor & Francis Group

ORIGINAL ARTICLE

Daily adaptive proton therapy – the key to innovative planning approaches for paranasal cancer treatments

Lena Nenoff[a,b], Michael Matter[a,b], Johanna Hedlund Lindmar[a,b], Damien Charles Weber[a,c,d], Antony John Lomax[a,b] and Francesca Albertini[a]

[a]Center for Proton Therapy, Paul Scherrer Institute, Villigen, Switzerland; [b]Department of Physics, ETH Zurich, Zurich, Switzerland; [c]Department of Radiation Oncology, University Hospital Zurich, Zurich, Switzerland; [d]Department of Radiation Oncology, University Hospital Bern, Bern, Switzerland

ABSTRACT

Background: For proton therapy of paranasal tumors, field directions avoiding volumes that might change during therapy are typically used. If the plan is optimized on the daily anatomy using daily adapted proton therapy (DAPT) however, field directions crossing the nasal cavities might be feasible. In this study, we investigated the effectiveness of DAPT for enabling narrow-field treatment approaches.

Material and methods: For five paranasal tumor patients, representing a wide patient spectrum, anatomically robust 4-field-star and narrow-field plans were calculated and their robustness to anatomical and setup uncertainties was compared with and without DAPT. Based on the nominal planning CTs, per patient up to 125 simulated CTs (simCTs) with different nasal cavity fillings were created and random translations and rotations due to patient setup uncertainties were further simulated. Plans were recalculated or re-optimized on all error scenarios, representing non-adapted and DAPT fractions, respectively. From these, 100 possible treatments (60 GyRBE, 30 fx) were simulated and changes in integral dose, target and organs at risk (OARs) doses evaluated.

Results: In comparison to the 4-field-star approach, the use of narrow-fields reduced integral dose between 29% and 56%. If OARs did not overlap with the target, OAR doses were also reduced. Finally, the significantly reduced target coverage in non-adapted treatments (mean V95 reductions of up to 34%) could be almost fully restored with DAPT in all cases (differences $<1\%$).

Conclusions: DAPT was found to be not only an effective way to increase plan robustness to anatomical and positional uncertainties, but also opened the possibility to use improved and more conformal field arrangements.

ARTICLE HISTORY
Received 25 March 2019
Accepted 26 June 2019

Introduction

Protons deliver highly conformal dose distributions to the target while sparing organs at risk (OARs). This allows dose escalation to the tumor and/or sparing of OARs for cases that are clinically challenging [1–4]. This comes at the cost of a high sensitivity to uncertainties along the beam path [5–9], such that changes in the patient anatomy or positioning can substantially affect the dose distribution [10]. One way to mitigate this effect is to adapt the treatment as soon as anatomical changes occur.

The importance of considering plan adaptation is widely recognized and several proton centers have defined adaptive workflow protocols [10–12]. If anatomical changes are expected, patients are regularly monitored with 3D imaging during treatment and, if necessary, the treatment is re-optimized offline. Typically, it takes a few days from image acquisition until a new plan is delivered, which is suboptimal for anatomical changes that vary on a daily basis (e.g. nasal cavity fillings). For such cases, the ideal approach would be a daily adapted proton therapy (DAPT), delivering a plan optimized every day based on a 3D, in-room image acquired directly before each fraction. With DAPT, both the daily anatomy *and* patient setup variations can be directly included in the daily plan optimization, allowing for reduced margins and irradiation of surrounding healthy tissue. As such, previous studies showed that a highly efficient DAPT workflow including the plan-of-the-day generation and validation might be feasible in less than five minutes after in-room 3D imaging [13,14].

In addition, DAPT could also enable the use of alternative field arrangements (e.g. narrow-angle approaches) which optimally minimize dose to healthy tissue, but is sensitive to anatomical changes without DAPT. In this study, we have investigated the potential advantage of a DAPT enabled narrow-angle approach for treating paranasal tumors, taking into account both anatomical and setup uncertainties.

CONTACT Lena Nenoff lena.nenoff@psi.ch WBBB 105, Forschungsstrasse 111, 5232 Villigen PSI, Switzerland

Supplemental data for this article can be accessed here.

Material and methods

Patient selection

Five paranasal patients, all previously treated with proton-therapy, were included in this work to cover the spectrum of tumor sizes, locations and initial nasal cavity fillings seen in our clinical practice (Figure 1). Patients 1 and 2 had both initially empty nasal cavities and very different tumor sizes; patients 3 and 4 had large tumor volumes in different locations, but half-filled cavities at their planning CTs; patient 5 had a moderately sized tumor and initially completely filled nasal cavities.

Plans

Intensity modulated proton therapy plans were optimized on the planning CT with an in-house developed planning system using the ray casting algorithm [15,16]. The Bragg peaks were positioned with a lateral spacing of 4 mm and water equivalent range separations of 2.5 mm (proximal spots) to 5.0 mm (deep spots). All plans were calculated to deliver a total dose of 60 GyRBE (RBE = 1.1) in 2 GyRBE/fraction.

Two field geometries were investigated: a 4-field-star approach and a narrow-field approach using three fields. The 4-field-star approach, consisting of two anteriorly and posteriorly inclined fields from the left and right, was optimized on a planning target volume (PTV) based on a homogeneous expansion of 5 mm around the clinical target volume (CTV), which is our current clinical practice. The narrow-field plans were calculated using field-specific PTVs generated by expanding the CTV isotropically by 1 mm and adding a range specific distal margin of 3%. With this, the patient setup was corrected for by the DAPT approach, allowing for the reduced PTV margin, while the 3% expansion in field direction deals with residual systematic range errors. The field angles were chosen to minimize the distance to the tumor from the patient surface, and therefore came predominantly from the anterior direction. Robust optimization was not used for any planning approach. Supplement 1 shows results of a pre-study analyzing the reduction of integral dose resulting from margin reduction *or* field geometry for patient 1.

Implementation of anatomical and setup changes

To simulate different cavity fillings, the planning CTs were modified to generate simulated CTs (simCTs) using an in-house developed program. Previously contoured left, right and central nasal cavities were first overwritten with an HU of –970 (air), with the internal voxels being then layer-wise overwritten with an HU of 30 to model mucus accumulation [17]. Depending on the volume of the nasal cavity, up to 125 simCTs were generated (125, 100, 48, 60 and 36 for patients 1–5, respectively). Potential daily setup errors were simulated by shifting each field's isocenter randomly along each cartesian axis using a standard deviation (σ) of 1.57 mm. This value was based on the residual intra-fractional movement of previously treated patients at our institute [18,19]. Similarly, rotational uncertainties were estimated based on our setup protocol, where rotations greater than 1.15° were typically corrected. As such, we assumed that 98% (2σ) of setups were within this angular error, leading to an σ of 0.57° for rotational setup errors. Rotational errors were randomly sampled from this Gaussian distribution and added to the planned gantry and couch rotations. Fraction doses were then generated by combining each simCT with five random translational and/or rotational error scenarios per simCT, leading to a pool of up to 625 anatomical and positioning scenarios per patient. Supplement 2 shows results of a pre-study evaluating the separate effects of setup *or* anatomical changes on treatment doses for patient 1.

Simulation of non-adapted and adapted treatments

The dosimetric effects of anatomical and setup uncertainties on each fraction of non-adapted treatments were estimated by *recalculating* the initial plans on different simulated daily scenarios, while DAPT fraction doses were simulated by *re-optimizing* each plan on the daily scenario, using the same margins, optimization constraints and field arrangements as the initial plan. From this database of fraction doses, treatment doses were generated by adding up 30 randomly selected fraction doses of the non-adapted and DAPT scenarios, respectively. This was repeated 100 times for each patient and plan geometry, simulating 100 non-adapted and DAPT treatments. This database of non-adapted and DAPT fraction doses (625, 500, 240, 300 and 180 for patients 1–5, respectively), allowed for the evaluation of a wide variety of possible treatments per patient and plan.

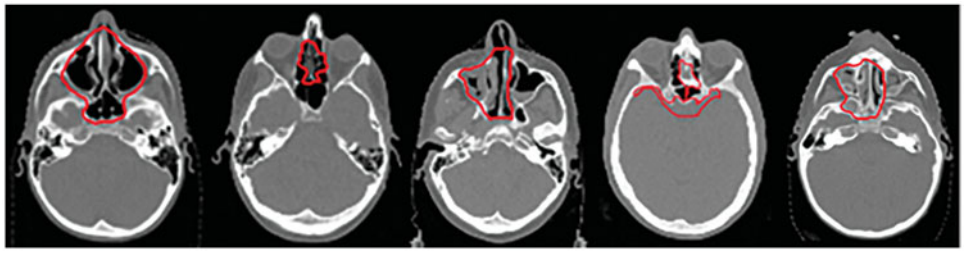

Figure 1. Representative slices of the five patients selected for this study. Patients 1 and 2 both had initially empty nasal cavities but large and small tumors, respectively. Patients 3 and 4 both had half filled cavities and large tumor. In addition, the tumor of patient 4 is partly located outside (posterior) the nasal cavities. For patient 5, the nasal cavities were initially filled.

Dose evaluation

For plan evaluation, healthy tissue integral dose and dose conformity indices (CIs) at the 95% and 50% isodoses ($V_{Isodose}/V_{Target}$, excluding dose in air) and CTV coverage as measured by V95 (the volume receiving 95% of the prescription dose) and D98 (the dose that 98% of the CTV receives) were considered. Sparing of relevant OARs (chiasma and brainstem) were evaluated and compared to each original treatment plan as reference. Statistical significance (5%) of differences between DAPT and non-adapted CTV parameters over all simulated treatments of each patient has been investigated with a paired, two sided Wilcoxon's signed rank test in Matlab (MathWorks, Natick, MA, USA).

Results

Differences in integral dose between the 4-field-star plan optimized with the clinical PTV, and the narrow-field approach with reduced field specific PTV, are shown in Table 1. For all patients, the narrow-field approach reduced integral dose of the initial plan by 29–56%. Additionally, the CI at the 50% isodose level (CI50%) was reduced by 17–46%, and CI10% by 33–60%.

Figure 2 shows the combined effect of anatomical and setup changes with and without DAPT for each patient. Without adaption, differences in CTV coverage were patient dependent. While for patient 2, a reduction in V95 of 34% in comparison to the nominal plan was observed, patient 5 showed only negligible differences. Despite these large variations, DAPT could restore the planned CTV coverage in all cases (V95 differences $<1\%$). Indeed, statistically significant differences between the non-adapted and DAPT treatments within patients in favor of adaption were observed in all CTV parameters.

OAR doses depended for both approaches mainly on the target and field geometry. The use of narrow-field approaches had a large potential to spare OARs. For instance, brainstem D2 was reduced in three out of five cases by up to 25% (patient 3), especially if the brainstem was close to the target. Similarly, in three out of five cases, the dose to the chiasma was reduced. For the remaining two cases, where the chiasm was attached to or surrounded by the target volume, a similar OAR sparing was achieved by both field approaches. Although DAPT did not recover OAR doses to those of the nominal plan, in most cases it provided improved organ sparing in all treatment simulations.

Discussion

We have compared treatment doses considering daily anatomical and setup variations with and without DAPT for two planning approaches. Our simulations demonstrated that DAPT mitigated daily positioning errors, allowing for substantial reduction of PTV margins, thus decreasing integral dose while preserving target coverage throughout the treatment (Figure 2). Moreover, we showed that DAPT enabled the use of nominally un-robust field arrangements, which could reduce the integral dose even further. For example, for patient 1, dose to healthy tissue decreased by 26% by using DAPT enabled margin reduction alone, and by 49% if combined with a narrow-field approach (Supplement 1). Over all patients, integral dose was reduced by 29–56% using the narrow-field approach combined with DAPT (Table 1).

We also demonstrated the dangers of this approach without DAPT. In the case of a plan optimized on empty, but applied to filled cavities, D98 to the CTV would reduce by up to 32% for the 4-field approach and by more than 51% for the narrow-field approach (Figure 3, patient 1). This was in line with previous work showing that the 4-field-star was relatively robust to anatomical changes [5].

Interestingly, variations in CTV coverage over the 100 sampled treatments were in some cases larger than 10% within individual patients, indicating the substantial and unpredictable effect of cavity changes on proton plans. The magnitude of these variations depended on the amount of cavity filling in the original planning CT. If the planning CT had empty cavities (patients 1 and 2), changes lead to distal under-dosage of the CTV and larger variations. Patients with initially half-filled cavities (patient 3), or with the CTV only partially overlapping with the cavities (patient 4), showed a less pronounced decrease. Patients with initially filled cavities (patient 5) were more robust in terms of CTV coverage but were more sensitive to potential overshoot into healthy tissue when the cavities emptied. With DAPT however, excellent target coverage was preserved for all planning approaches, even with substantially reduced PTV margins (see Figure 2).

Clearly, our non-adapted simulations were a worst-case approximation. Typically, for paranasal tumors, regular on-treatment-CTs are clinically acquired such that plans could be adapted within a few days [10]. Nevertheless, DAPT is the best solution to mitigate such changes, especially those that occur on a daily basis. In addition, daily optimization of the plan could help exploit anatomies that are more favorable for treatment. For instance, if the cavities were empty in the initial CT, sharp bone/air interfaces locally distorted the Bragg peak, potentially affecting both the conformation and

Table 1. Integral dose and conformity index at 50% and 10% isodose level of the 4-field-star initial treatment plans with homogeneous margin and the narrow-field plans with reduced margin.

	Integral dose/Gy*l		CI10		CI50	
Patient	Narrow-field	4-Field-star	Narrow-field	4-Field-star	Narrow-field	4-Field-star
1	24.0	45.7	3.6	6.4	2.3	3.3
2	6.3	13.5	10.5	26.2	4.5	6.7
3	12.3	27.8	5.0	12.5	2.9	4.5
4	19.8	28.0	10.4	15.5	5.2	6.3
5	33.2	51.8	5.2	7.8	3.1	3.8

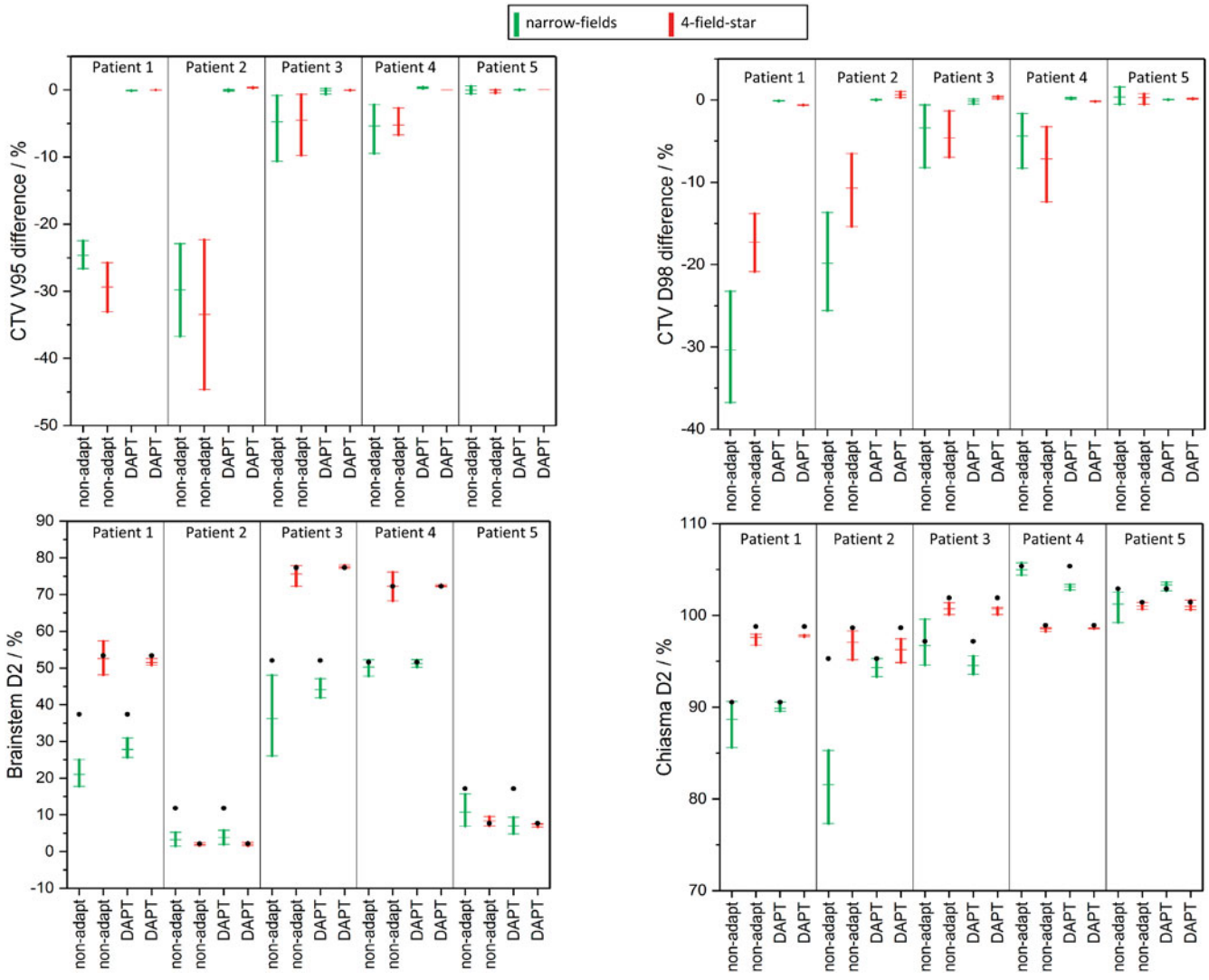

Figure 2. Differences in CTV D98, V95 and selected OAR parameters of 100 simulated treatments for the narrow-field plan with reduced margin and the 4-field-star with clinical PTV margin. Parameters from original plans are marked with circles. Outliers are marked with red crosses. CTV D98 and V95 for the non-adapted and daily adapted treatments doses differ significantly (significance level 5%).

homogeneity of dose to the target volume. If the cavities filled during treatment however, density heterogeneity reduced, resulting in a more conformal and homogenous dose to the tumor and improved sparing of OAR (see Figure 2).

Variable cavity fillings in this study were modeled using artificially modified CTs [17], assuming an equally distributed probability for each filling scenario, resulting in drastic day-to-day changes. Although observed for some patients at our clinic, such changes could be considered as a worst-case scenario. In addition, irregular cavity filling, patient weight changes or tumor growth/shrinkage were not considered. However, there is no reason to believe that these could not also be compensated using a DAPT approach as demonstrated here for variable cavity filling. Finally, it was demonstrated that even if the patient anatomy did not change during treatment, with a DAPT approach the patient would still benefit from reduced integral dose.

As all beams came from the anterior direction, they also all stopped in the posterior area of the target volume, and regions of enhanced linear energy transfer (LET) from all beams were therefore concentrated in this same region. This was in contrast to the 4-field-star approach, where the beams came equally from both sides of the patient and distributed and diluted regions of enhanced LET around the periphery of the target volume. As such, the narrow-field approach might be more sensitive to distal end biological effects. This could be dealt possibly by reducing healthy tissue tolerances to distally positioned OARs, or by including LET into the optimization to re-distribute it away from critical organs [20].

We acknowledge that alternative methods to mitigate anatomical and positional changes have been suggested. Some authors proposed to include anatomical changes directly in the optimization algorithm by including multiple CT scenarios [17,21] or to adjust daily patient positioning to reduce the differences between planned and daily dose in the presence of anatomical changes [22]. However, Van De Water et al. [17] compared, for the same field arrangement, the robustness of anatomically robust optimized and daily

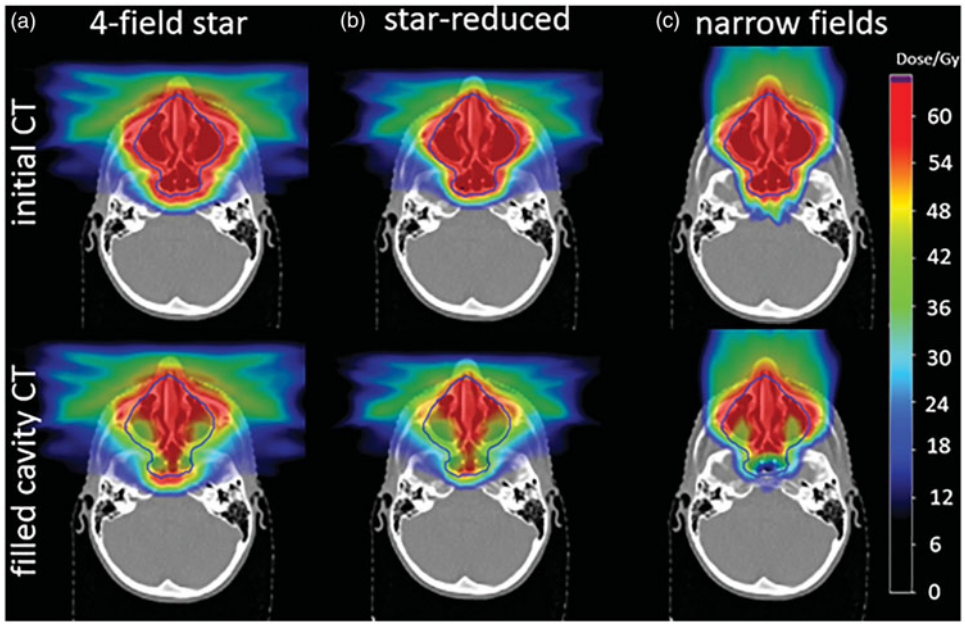

Figure 3. Initial plan calculated on the empty planning CT (top) and recalculated plan on filled cavity CT (bottom) for patient 1 with (a) 4-field-star arrangement with homogeneous PTV, (b) 4-field-star with field specific PTV and (c) narrow-field arrangement with field-specific PTV.

adapted proton plans. They demonstrated that, even though using an anatomical robust optimization was a valid strategy to mitigate the effect of anatomy, DAPT, even without the added benefits of a more conformal beam approach, had the advantage of reducing integral dose and improving dose conformability compared to robust optimization.

The clinical implementation of DAPT presents some challenges, for instance daily 3D imaging with high enough quality for replanning as well as contour propagation, fast plan optimization, measurement free quality assurance (QA) and accurate dose accumulation across multiple 3D data sets.

For daily imaging, there are three possibilities: In-room CT, cone beam CT (CBCT) or on-board MR imaging. The use of in-room CT currently guarantees the most accurate definition of proton stopping power, and with a low-dose protocol, it is possible to limit the imaging dose to the patient to below 1 mGy per CT [23,24], similar to that delivered with CBCT [25]. CBCT for adaption is currently under investigation but extracting density information with the same accuracy as with CT [26–30] remains challenging. The use of MRI for daily imaging clearly has advantages of no imaging dose, but is currently only under investigation [31,32].

As for fast planning and plan QA, we have previously demonstrated that the complete optimization of plans can be performed in just a few seconds [13], whereas efficient independent dose calculations, based on machine control files, provided a fast and sensitive alternative to plan specific QA measurements [14,33]. Finally, although accurate contour propagation and dose accumulation for deformable geometries are still challenging [34], for the paranasal sinuses spatial transformations between daily datasets are predominantly rigid, simplifying both processes considerably. As such, we believe that a highly efficient, DAPT workflow for the treatment site investigated in this work is a realistic prospect in the near future.

In conclusion, daily plan adaptation has been demonstrated to be a useful technique to mitigate anatomical changes, and could be the key for enabling the safe use of improved field arrangements for proton therapy that would normally be considered un-robust.

Disclosure statement

No potential conflict of interest was reported by the authors.

Funding

We acknowledge the Swiss National Science Foundation (grant project: 320030 165961) for their support.

ORCID

Lena Nenoff http://orcid.org/0000-0002-7468-835X
Michael Matter http://orcid.org/0000-0002-2612-3207

References

[1] Weber DC, Schneider R, Goitein G, et al. Spot scanning-based proton therapy for intracranial meningioma: long-term results from the Paul Scherrer Institute. Int J Radiat Oncol Biol Phys. 2012;83:865–871.
[2] Verma V, Lin SH, Simone CB, et al. Clinical outcomes and toxicities of proton radiotherapy for gastrointestinal neoplasms: a systematic review. J Gastrointest Oncol. 2016;7:644–664.
[3] Pehlivan B, Ares C, Lomax AJ, et al. Temporal lobe toxicity analysis after proton radiation therapy for skull base tumors. Int J Radiat Oncol Biol Phys. 2012;83:1432–1440.
[4] Weber DC, Badiyan S, Malyapa R, et al. Long-term outcomes and prognostic factors of skull-base chondrosarcoma patients treated with pencil-beam scanning proton therapy at the Paul Scherrer Institute. Neuro Oncol. 2016;18:236–243.

[5] Albertini F, Casiraghi M, Lorentini S, et al. Experimental verification of IMPT treatment plans in an anthropomorphic phantom in the presence of delivery uncertainties. Phys Med Biol. 2011;56:4415–4431.
[6] Albertini F, Bolsi A, Lomax AJ, et al. Sensitivity of intensity modulated proton therapy plans to changes in patient weight. Radiother Oncol. 2008;86:187–194.
[7] Kraan AC. Range verification methods in particle therapy: underlying physics and Monte Carlo modeling. Front Oncol. 2015;5:1–27.
[8] Knopf A-C, Lomax A. In vivo proton range verification: a review. Phys Med Biol. 2013;58:R131–R160.
[9] Schaffner B, Pedroni E, Lomax A. Dose calculation models for proton treatment planning using a dynamic beam delivery system: an attempt to include density heterogeneity effects in the analytical dose calculation. Phys Med Biol. 1999;44:27–41.
[10] Placidi L, Bolsi A, Lomax AJ, et al. The effect of anatomical changes on pencil beam scanned proton dose distributions for cranial and extra cranial tumors. Int J Radiat Oncol Biol Phys. 2017;97:616–623.
[11] Stock M, Georg D, Ableitinger A, et al. The technological basis for adaptive ion beam therapy at MedAustron: status and outlook. Z Med Phys. 2018;28:196–210.
[12] Stützer K, Jakobi A, Bandurska-Luque A, et al. Potential proton and photon dose degradation in advanced head and neck cancer patients by intratherapy changes. J Appl Clin Med Phys. 2017;18:104–113.
[13] Matter M, Nenoff L, Meier G, et al. IMPT plan generation in under ten seconds on a GPU. Acta Oncol. [cited 2019 Jul 4]; [5 p.]. DOI:10.1080/0284186X.2019.1630753.
[14] Matter M, Nenoff L, Meier G, et al. Alternatives to patient specific verification measurements in proton therapy: a comparative experimental study with intentional errors. Phys Med Biol. 2018;63:205014.
[15] Winterhalter C, Zepter S, Shim S, et al. Evaluation of the ray-casting analytical algorithm for pencil beam scanning proton therapy. Phys Med Biol. 2019;64:065021.
[16] Schaffner B, Pedroni E, Lomax A. Dose calculation models for pro-ton treatment planning using a dynamic beam delivery system:an attempt to include density heterogeneity effects in the analytical dose calculation. Phys Med Biol. 1999;44:27–41.
[17] Van De Water S, Albertini F, Weber DC, et al. Anatomical robust optimization to account for nasal cavity filling variation during intensity-modulated proton therapy: a comparison with conventional and adaptive planning strategies. Phys Med Biol. 2018;63:025020.
[18] Bolsi A, Lomax AJ, Pedroni E, et al. Experiences at the Paul Scherrer Institute with a remote patient positioning procedure for high-throughput proton radiation therapy. Int J Radiat Oncol. 2008;71:1581–1590.
[19] Lowe M, Albertini F, Aitkenhead A, et al. Incorporating the effect of fractionation in the evaluation of proton plan robustness to setup errors. Phys Med Biol. 2016;61:413–429.
[20] Grassberger C, Trofimov A, Lomax A, et al. Variations in linear energy transfer within clinical proton therapy fields and the potential for biological treatment planning. Int J Radiat Oncol Biol Phys. 2011;80:1559–1566.
[21] Wang X, Li H, Zhu XR, et al. Multiple-CT optimization of intensity-modulated proton therapy – is it possible to eliminate adaptive planning? Radiother Oncol. 2018;128:167–173.
[22] Kurz C, Süss P, Arnsmeyer C, et al. Dose-guided patient positioning in proton radiotherapy using multicriteria-optimization. Z Med Phys. 2018.
[23] Smith-Bindman R, Lipson J, Marcus R, et al. Radiation dose associated with common computed tomography examinations and the associated lifetime attributable risk of cancer. Arch Intern Med. 2009;169:2078–2086.
[24] Lin EC. Radiation risk from medical imaging. Mayo Clin Proc. 2010;85:1142–1146.
[25] Buckley JG, Wilkinson D, Malaroda A, et al. Investigation of the radiation dose from cone-beam CT for image-guided radiotherapy: a comparison of methodologies. J Appl Clin Med Phys. 2018;19:174–183.
[26] Kurz C, Dedes G, Resch A, et al. Comparing cone-beam CT intensity correction methods for dose recalculation in adaptive intensity-modulated photon and proton therapy for head and neck cancer. Acta Oncol. 2015;54:1651–1657.
[27] Kurz C, Nijhuis R, Reiner M, et al. Feasibility of automated proton therapy plan adaptation for head and neck tumors using cone beam CT images. Radiat Oncol. 2016;11:1–9.
[28] Landry G, Hansen D, Kamp F, et al. Comparing Unet training with three different datasets to correct CBCT images for prostate radiotherapy dose calculations. Phys Med Biol. 2019;64:035011.
[29] Kurz C, Kamp F, Park Y-K, et al. Investigating deformable image registration and scatter correction for CBCT-based dose calculation in adaptive IMPT. Med Phys. 2016;43:5636–5646.
[30] Hansen DC, Landry G, Kamp F, et al. ScatterNet: a convolutional neural network for cone-beam CT intensity correction. Med Phys. 2018;45:4916–4926.
[31] Koivula L, Wee L, Korhonen J. Feasibility of MRI-only treatment planning for proton therapy in brain and prostate cancers: dose calculation accuracy in substitute CT images. Med Phys. 2016;43:4634–4642.
[32] Moteabbed M, Schuemann J, Paganetti H. Dosimetric feasibility of real-time MRI-guided proton therapy. Med Phys. 2014;41:111713.
[33] Winterhalter C, Fura E, Tian Y, et al. Validating a Monte Carlo approach to absolute dose quality assurance for proton pencil beam scanning. Phys Med Biol. 2018;63:175001.
[34] Ribeiro CO, Knopf A, Langendijk JA, et al. Assessment of dosimetric errors induced by deformable image registration methods in 4D pencil beam scanned proton treatment planning for liver tumours. Radiother Oncol. 2018;128:174–181.